Journal of
Materials Chemistry A

Materials for energy and sustainability

www.rsc.org/MaterialsA

H$_2$

H$_2$

H$_2$
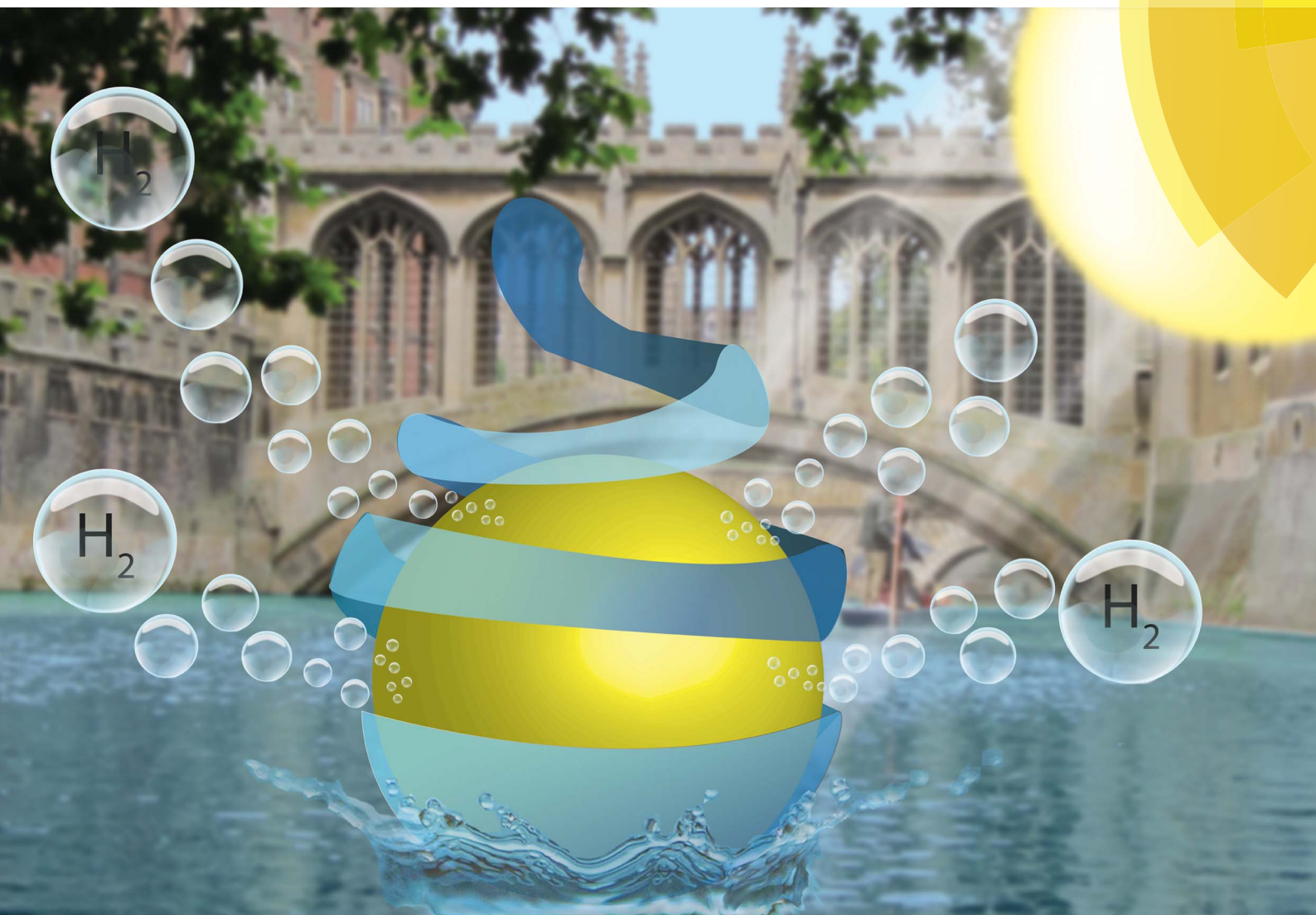
Themed issue: Water splitting and photocatalysis

ROYAL SOCIETY
OF CHEMISTRY

PAPER
Erwin Reisner *et al.*
Ligand removal from CdS quantum dots for enhanced photocatalytic
H$_2$ generation in pH neutral water

175 YEARS

Ligand removal from CdS quantum dots for enhanced photocatalytic H$_2$ generation in pH neutral water†

Christina M. Chang,‡ Katherine L. Orchard,‡ Benjamin C. M. Martindale and Erwin Reisner*

Ligand-free CdS quantum dots were produced by a reactive ligand stripping procedure and employed for photocatalytic H$_2$ evolution in pH neutral solution. The rate of H$_2$ generation of the 'bare' quantum dots was 175 times higher than that of the equivalent mercaptopropionic acid-capped quantum dots in the presence of a cobalt co-catalyst and Na$_2$SO$_3$ as a sacrificial electron donor. Under optimised conditions, a turnover number of 58 000 mol H$_2$ per mol Co and 29 000 mol H$_2$ per mol CdS quantum dots was achieved after 88 h of UV-free solar light irradiation (λ > 420 nm, 1 Sun intensity). Ligand removal is therefore a potent method to substantially enhance the photocatalytic performance of quantum dot systems.

Introduction

Converting the energy in sunlight into chemical fuels is a potential solution to meet our need for sustainable energy storage.[1–3] Many synthetic systems have been developed with the hope of emulating natural photosynthesis to produce renewable fuels such as H$_2$. Such artificial photosynthetic systems typically consist of a photosensitiser – such as a molecular dye or a semiconductor (nano)particle – coupled to an inorganic, organometallic or enzymatic catalyst, which carries out the fuel-producing redox reaction.[4–7]

Semiconductor quantum dots (QDs) are well suited as light absorbers for photocatalysis due to their high light absorption coefficient, high surface area, tuneable optical and electronic properties, and relatively high photostability compared to molecular dyes.[7–9] Although photocatalytic H$_2$ generation systems using bulk and nanostructured metal chalcogenides have been studied for many years,[10–15] systems using QDs have been pioneered only relatively recently, employing CdX (X = S, Se, Te) QDs coupled to a wide range of co-catalysts, including noble metals,[16,17] enzymes,[18–21] and molecular complexes or salts of iron,[22–24] cobalt,[25–27] and nickel.[28,29]

The most active QD-based photocatalytic systems to date operate under either acidic (pH < 5),[22–29] or highly alkaline conditions (pH ≥ 11),[30] with greatly reduced activity around neutral pH. However, activity close to pH 7 is important for developing sustainable technologies in which, ultimately, river water or seawater could be employed. In addition, enzymes and some synthetic electrocatalysts such as the cobaloxime **CoP** (Fig. 1) and semiconductor light absorbers such as BiVO$_4$ (for use in tandem with a QD for full water splitting) display optimal activity around pH 7.[18,31,32] Therefore, extending the utility of QDs to neutral conditions is an important goal.

QDs used in photocatalytic systems have previously been functionalised with hydrophilic, thiol-based ligands, such as thioglycolic acid (TGA), 3-mercaptopropionic acid (MPA), or dihydrolipoic acid (DHLA), in order to prevent aggregation and to induce solubility in aqueous solution. However, these capping ligands are not innocent and have been proposed to have secondary roles such as acting as a physical[33] or electronic barrier.[34] They have also been shown to interfere with co-catalysts by denaturing enzymes,[19] and by altering metal-based

Department of Chemistry, University of Cambridge, Lensfield Road, Cambridge CB2 1EW, UK. E-mail: reisner@ch.cam.ac.uk; Web: http://www-reisner.ch.cam.ac.uk

† Electronic supplementary information (ESI) available: Additional figures, tables, and experimental details. See DOI: 10.1039/c5ta04136h. Additional data related to this publication is available at the University of Cambridge data repository (https://www.repository.cam.ac.uk/handle/1810/248732).

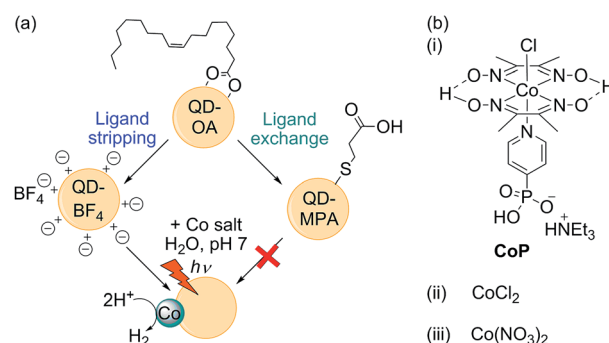‡ These authors contributed equally.

Fig. 1 (a) Schematic representation of the preparation and relative activity of the CdS QDs used in this study; (b) (i) structure of the molecular catalyst **CoP**, and (ii and iii) the two cobalt salts used as co-catalysts.

2856 | *J. Mater. Chem. A*, 2016, 4, 2856–2862

This journal is © The Royal Society of Chemistry 2016

molecular catalysts to form complexes that are either more active (for Ni^{2+})[28] or inactive (for Co^{2+}).[27] Moreover, the affinity of thiol ligands for CdX surfaces decreases with decreasing pH,[35,36] such that the ligands desorb more readily under commonly-used acidic photocatalytic conditions.

Whereas previous work has sought to improve QD photo-activity at low pH by increasing the binding affinity of the capping ligands,[27] here we take the opposite approach and demonstrate that QD activity at neutral pH is dramatically improved by complete removal of the surface ligands. We propose that desorption of surface capping groups is integral to QD/catalyst activity and show that the use of bare QDs results in a two orders of magnitude increase in catalytic rate compared to the equivalent MPA-capped QD/catalyst system.

Experimental section

General materials and methods

Unless otherwise stated, reagents were purchased from commercial suppliers and used as received with the following purities: CdO (99.998%), sulfur (99.998%), oleic acid (OA, 90%), octadecene (ODE, 90%), 3-mercaptopropionic acid (MPA, ≥99%), tetramethylammonium hydroxide, pentahydrate (TMAOH, 99%), trimethyloxonium tetrafluoroborate (96%), sodium sulfite (≥98%), cobalt(II) chloride hexahydrate (98%). Anhydrous solvents were purchased from Acros Organics with the following purities: $CHCl_3$ (99.9%), dimethylformamide (DMF, 99.8%), acetonitrile (ACN, 99.9%). All other organic solvents used were HPLC grade. All aqueous solutions were prepared with distilled water. $(Et_3NH)[Co^{III}Cl(dmgH)_2(pyridyl-4-hydrophosphonate)]$ (**CoP**) was prepared according to a literature procedure.[37] Unless otherwise stated, all experiments were carried out in air. Na_2SO_3 buffer solutions were titrated with dilute HCl to the desired pH value at 25 °C.

Synthetic procedures

QD-OA. CdS QDs capped with oleic acid ligands (QD-OA) were prepared according to a previously reported procedure.[16] Briefly, a mixture of CdO (0.64 g) and OA (26 g) in ODE (70 g) was heated under Ar atmosphere to 280 °C. Sulfur (0.08 g) in ODE (30 g) was added rapidly and the solution was allowed to cool to 250 °C. This temperature was maintained for 120 s before quenching by rapid cooling. The particles were precipitated from 1 : 1 hexane : methanol using excess acetone, centrifuged at 7000 rpm for 3 min, and re-dispersed in hexane. Two further washing steps were carried out using hexane and acetone as solvent and non-solvent, respectively, before finally dispersing in hexane (20 mL).

QD-MPA. Ligand exchange with MPA was carried out according to a literature procedure.[35] MPA (0.5 mL) was dispersed in 1 : 1 chloroform : methanol (10 mL) and the pH was adjusted to 11 with TMAOH. QD-OA solution (2 mL) was added to this mixture and stirred in the dark for two days. The QDs were precipitated with excess acetone and centrifuged (7000 rpm, 3 min). The isolated particles were washed with acetone before being dispersed in water (1 mL).

QD-BF₄. The reactive ligand stripping was carried out using a modified literature procedure.[38] QD-OA solution in hexane (1 mL) was evaporated to dryness and, under N_2 atmosphere, re-dispersed in a mixture of anhydrous $CHCl_3$ (3 mL) and anhydrous DMF (0.2 mL). Aliquots of stripping agent (Me_3OBF_4, 1.0 M in ACN) were added slowly until the particles precipitated (typically ∼0.9 mL). The stripped particles were centrifuged (7000 rpm, 3 min), dried in air for 1 min, and re-dispersed in DMF (1–2 mL).

QD-BF₄ "re-capping" procedure. An MPA solution (0.5 mL, in methanol) was prepared and adjusted to pH 11 with TMAOH. Aliquots of this solution (600 μL total) were added to a solution of QD-BF₄ in DMF (1 mL, 43 μM), forming an opaque suspension. Methanol (300 μL) was added to form a yellow, transparent solution, which was stirred, protected from light, for a further 1 h. The particles were precipitated with excess acetone and isolated by centrifugation (7000 rpm, 3 min). The particles were washed with acetone before dispersing in water (150 μL).

Photocatalysis experiments

Assembly of photocatalysis system. In general, CdS QD and co-catalyst solutions were added sequentially to a Na_2SO_3 solution at the required concentration and pH to give a final volume of 2.5 mL. Photocatalysis was carried out in Pyrex pressure vessels with a headspace of either 2.1 or 5.2 mL, sealed tightly with a rubber septum; the volume of the headspace did not affect the measured volume of H_2. A typical procedure is as follows: QD-BF₄ (48 μL, 104 μM in DMF) and $CoCl_2$ (50 μL, 0.2 mM in H_2O) were added to Na_2SO_3 (2.4 mL, 0.1 M, pH 7). The vessel was sealed, protected from light, and purged for at least 10 min with 2% CH_4 in N_2 before photocatalysis experiments began. CH_4 provided an internal standard for H_2 measurement (see below). The DMF content of the solution was typically between 1–3% v/v. For experiments with commercial CdS, the same preparation as above but with 0.6 mg CdS was used in each sample, in line with the calculated mass of CdS employed for the QDs.

Photocatalytic studies. Samples were irradiated using a calibrated solar light simulator (Newport Oriel, 100 mW cm^{-2}) equipped with an air mass 1.5 global filter. Infrared and ultraviolet irradiation were filtered using a water filter (10 cm path length) and a 420 nm long-pass filter (UQG Optics), respectively. The reaction vessel temperature was kept constant at 25 °C with a water jacket connected to a temperature-controlled circulator. Evolved H_2 was measured by taking aliquots (20 μL) of the headspace gas and analysing them using an Agilent 7890A Series Gas Chromatograph (GC) equipped with a 5 Å molecular sieve column (N_2 carrier gas at a flow rate of approximately 3 mL min^{-1}). The column temperature was kept at 45 °C, and a thermal conductivity detector was used. The GC was calibrated for H_2 regularly using gas titration of known $H_2/CH_4/N_2$ mixtures. Unless otherwise stated, data presented is given as the mean of three independent experiments, with errors given as ±1 standard deviation (σ) or ±10% of the mean, whichever is greater.

This journal is © The Royal Society of Chemistry 2016

J. Mater. Chem. A, 2016, **4**, 2856–2862 | **2857**

Long-term irradiation study. Photocatalysis solutions ([QD-BF$_4$] = 2 µM, [CoCl$_2$] = 4 µM, 1.0 M Na$_2$SO$_3$, pH 7) were irradiated for 44 h, with purging after each 12 h interval to prevent excessive pressure build-up. After this time, the vessels were opened and the pH adjusted *in situ* using 1.0 M HCl. The solutions were purged and irradiated for a further 22 h. After this time, the vessels were opened and fresh Na$_2$SO$_3$ (113 mg) added. The pH was adjusted using concentrated HCl, the solutions purged, and irradiated for a further 22 h.

Re-suspension experiments. Photocatalysis solutions ([QD-BF$_4$] = 2 µM, [CoCl$_2$] = 4 µM, 0.1 M Na$_2$SO$_3$, pH 7) were irradiated for 4 h then isolated by centrifugation (10 000 rpm, 10 min). The supernatant was separated and the precipitate washed by re-suspending in water (2 mL) followed by centrifugation (10 min). The precipitate was then suspended in fresh Na$_2$SO$_3$ (0.1 M, pH 7), purged with 2% CH$_4$ in N$_2$ and irradiated for a further 4 h. To avoid any deleterious effects of exposure to air, the isolation and re-suspension procedure was carried out in a nitrogen-filled glovebox.

Results and discussion

Synthesis and surface modification of CdS QDs

As outlined in Fig. 1, oleic acid-capped CdS QDs (QD-OA) were synthesised by a hot injection method,[16] and used to prepare both MPA-capped particles (QD-MPA) and ligand-free, charge-stabilised QDs (QD-BF$_4$). QD-MPA were prepared following a standard ligand exchange procedure by treating QD-OA with MPA in basic solution.[35] QD-BF$_4$ were prepared following a modified reactive ligand stripping procedure, using [Me$_3$O]BF$_4$ in the presence of dimethylformamide (DMF) to remove the oleic acid groups.[38] The ligand stripping process yields well-dispersed individual particles when suspended in polar solvents such as DMF and dimethyl sulfoxide (Fig. S1† for transmission electron microscopy, TEM, image).

Fourier transform infrared spectroscopy (FT-IR) of dried QD-BF$_4$ revealed resonances from DMF and (BF$_4$)$^-$, which are the expected surface groups following ligand stripping (Fig. S2†). Ligand stripping did not affect the CdS crystal phase (Fig. S3† for powder X-ray diffraction, XRD), but the absorption maximum changed from λ_{max} = 443 nm to 427 nm (Fig. S4† for UV-vis spectra). This blue-shift corresponds to a decrease in the CdS QD particle size from 5.0 nm to 4.2 nm,[39] which is in agreement with TEM measurements (4.5 ± 0.5 nm for QD-OA and 4.1 ± 0.6 nm for QD-BF$_4$). The (BF$_4$)$^-$ anion is known to etch CdTe QDs,[40] and therefore a similar etching process is a likely reason for the reduced size of QD-BF$_4$.

Photocatalysis experiments

Photocatalysis solutions were prepared by sequentially adding stock solutions of QDs and either **CoP**, CoCl$_2$ or Co(NO$_3$)$_2$ to a stirred, aqueous solution of the sacrificial electron donor (0.1 M Na$_2$SO$_3$, pH 7). Whereas QD-MPA formed a stable suspension that did not precipitate over the course of the photocatalysis experiment, QD-BF$_4$ rapidly formed a visibly hazy suspension that precipitated if not stirred. FT-IR of QD-BF$_4$ precipitated

from aqueous solution shows significantly reduced (BF$_4$)$^-$ resonances (Fig. S2†), indicating that most of the counter ions are dissolved in water. Under visible light irradiation (air mass 1.5 G filter, 100 mW cm^{-2}, λ > 420 nm), QD-MPA produced negligible amounts of H$_2$ in the presence and absence of cobalt co-catalysts (Fig. 2, Tables 1 and S1†). In contrast, QD-BF$_4$ was over 60 times more active than QD-MPA, and its activity was further enhanced tenfold by the addition of cobalt species.

To control for the reduced particle size of QD-BF$_4$ compared to QD-MPA, we capped QD-BF$_4$ with MPA ('re-capped' QDs) and compared the activity. The H$_2$ evolution yield of the 're-capped' dots with CoCl$_2$ remained significantly lower than that of the bare QD-BF$_4$ (1.53 ± 0.42 and 32.8 ± 4.9 µmol after 4 h irradiation, respectively; Table S1†), confirming that the primary activity enhancing effect of ligand stripping stems from the lack of MPA surface groups in QD-BF$_4$ and not the decrease in QD size. Furthermore, the presence of small amounts of DMF in the QD-BF$_4$ solutions is not a contributing factor to the difference in activity between QD-BF$_4$ and QD-MPA, since adding an equivalent quantity of DMF to QD-MPA solutions did not influence the activity. Equivalent experiments with commercial CdS (Sigma-Aldrich, 0.6 mg) yielded activity on the same order of magnitude as that of QD-MPA (Table S1,† entry 10). From these results we infer that both the small particle size and the bare CdS surface are necessary for high activity.

The observed photocatalytic activity was independent of the Co species used as co-catalyst (Fig. 1, 2 and Table S1†), which suggests that the same active species is formed in each case. Although **CoP** has been shown to act as a molecular catalyst on dye-sensitised TiO$_2$,[41,42] cobaloximes are known to partially dissociate from a surface or light absorber,[42–45] and to fully decompose under highly reducing conditions.[46,47] The presence of an induction period followed by linear photostability over hours is in contrast to the behaviour of **CoP** on dye-sensitised TiO$_2$, and is consistent with decomposition to form a catalytically active deposit.[48] We therefore propose that **CoP** is photo-decomposed during an initial activation period, which may result from the high driving force provided by the CdS
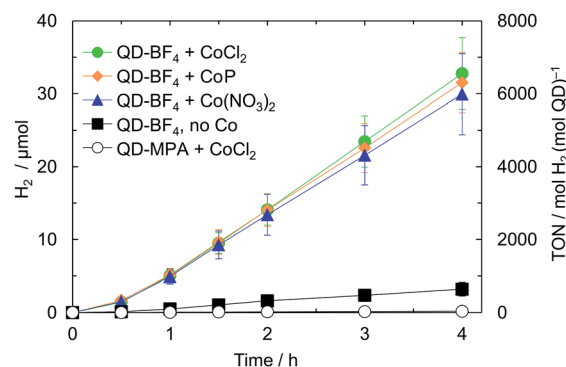

Fig. 2 Comparison of visible-light driven H$_2$ evolution performance with mercaptopropionic acid-capped CdS (QD-MPA) and ligand-stripped CdS (QD-BF$_4$) in the presence of various Co co-catalysts at 25 °C (0.1 M Na$_2$SO$_3$, pH 7, [QD-BF$_4$] = 2 µM, [Co] = 4 µM, 2.5 mL, irradiation λ > 420 nm, 100 mW cm^{-2}).

Table 1 Visible light-driven H_2 evolution with QD–MPA and QD–BF$_4$ in the presence and absence of CoCl$_2$[a]

System[a]	$H_2/\mu mol$	TOF_{QD}[b] $\pm \sigma/h^{-1}$	TOF_{Co}[c] $\pm \sigma/h^{-1}$
QD-MPA	0.05 ± 0.02	2.63 ± 0.88	—
QD-MPA/CoCl$_2$	0.19 ± 0.03	9.36 ± 1.42	4.68 ± 0.71
QD-BF$_4$	3.22 ± 0.95	161 ± 48	—
QD-BF$_4$/CoCl$_2$	32.8 ± 4.9	1639 ± 246	819 ± 123

[a] Values reported for H_2 produced after 4 h irradiation at 25 °C ($\lambda > 420$ nm, 100 mW cm^{-2}, [QD] = 2 µM, [Co] = 4 µM, 0.1 M Na$_2$SO$_3$, pH 7, 2.5 mL). [b] Turnover frequency per QD, TOF_{QD}, in mol H_2 per mol QD per h. [c] Turnover frequency per Co, TOF_{Co}, in mol H_2 per mol Co per h.

Fig. 3 Long-term photoactivity of the optimised QD–BF$_4$/CoCl$_2$ system at 25 °C ([QD–BF$_4$] = 2 µM, [Co] = 4 µM, 1.0 M Na$_2$SO$_3$, pH 7, $\lambda > 420$ nm, 100 mW cm^{-2}).
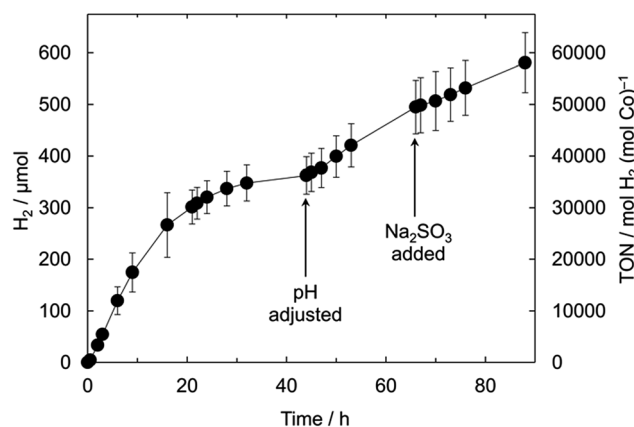
conduction band (values reported range from −1.7 V to −0.7 V *vs.* NHE, depending on surface properties and QD diameter).[49]

The photocatalytic QD–BF$_4$ system was optimised using CoCl$_2$ as the co-catalyst. A [QD] : [Co] ratio of 1 : 2, with [QD] = 2 µM, and [Na$_2$SO$_3$] of 1.0 M was found to give optimal H_2 evolution activity (Fig. S5–S7 and Table S2† entry 12). A five-fold higher loading of Co did not increase the activity with respect to the QDs. The external quantum efficiency (EQE) of the QD–BF$_4$/CoCl$_2$ system at $\lambda = 420$ nm was 7.7 ± 1.4% and remained approximately constant over 3 h (see ESI for details†).

The photocatalytic activity is highly sensitive to the solution pH with a clear maximum in activity at pH ∼ 7 (Fig. S8†). The optimum pH correlates with the pK_a of the sacrificial electron donor (7.2 for HSO$_3^-$),[50] but may also be related to other factors such as the degree of protonation of the particle surfaces and the corresponding changes in the QD conduction and valence band energies or a pH-dependent quantum yield of generated photo-reduced species.[30,51,52] This pH sensitivity of the QD–BF$_4$/CoCl$_2$ hybrid system was found to be the main factor limiting the long-term stability of the system (Fig. 3). Under continuous solar light illumination ($\lambda > 420$ nm), the H_2 evolution ceased after approximately 44 h, where a pH of 11.3 ± 0.1 was measured. Adjusting the solution pH again to pH 7 with aqueous HCl restored much of the initial rate of H_2 evolution. The activity was not fully restored to the initial rate, which may be due to degradation of the QDs by repeated exposure to air, alkaline solution and/or HCl (for pH adjustment). In contrast, adding Na$_2$SO$_3$ did not cause an increase in activity. After 88 h irradiation, 581 ± 58 µmol H_2 was produced, corresponding to a TON_{Co} of 58 000 ± 5800 and TON_{QD} of 29 000 ± 2900. QD–BF$_4$/CoCl$_2$ is the most active QD/catalyst system at pH 7 to date, with activity on par with – or higher than – the related photocatalytic microstructured nanoparticle/co-catalyst aggregates, formed from MPA-capped CdTe QDs and CoCl$_2$ at pH 4.65 (Table S3†).[25]

Characterisation of the active catalyst

Inductively-coupled plasma-optical emission spectroscopy (ICP-OES) of both the particles and supernatant isolated from a QD–BF$_4$/CoCl$_2$ solution after 4 h irradiation showed that 87% of the detected Co is attached to the QDs, with a calculated Co loading of ∼0.1 wt% (Table S4†). It is notable that the measured Co content on QD–BF$_4$ is similar to that of the related CdTe/CoCl$_2$

system (0.15 wt%),[25] but that the required amount of CoCl$_2$ in solution for our system is much lower, presumably due to the ligand-free CdS surface (2 equivalents per QD in this work compared to 1000 equivalents for CdTe/CoCl$_2$). The TON_{Co} based on total added Co is therefore much higher for our system (TON_{Co} 30 000 after 21 h *cf.* 86 for CdTe/CoCl$_2$; Table S3†).

Particles isolated from a QD–BF$_4$/CoP solution were found to have a similar Co loading to that of QD–BF$_4$/CoCl$_2$ (Table S4†), supporting the hypothesis that the nature of the active catalyst is independent of the Co species. Additionally, Co was not detected in particles isolated from either QD–MPA/CoCl$_2$ or 're-capped' QD–BF$_4$/CoCl$_2$ solutions, indicating that integration of Co into the particles is necessary for high photocatalytic activity.

Particles isolated from the photocatalysis solution and re-suspended in fresh Na$_2$SO$_3$ retained 90% of their activity (no additional Co, Fig. S9†), confirming that the CdS/Co particles are the active species. An induction period was observed within the first 30 min of irradiation (Fig. 2), indicating that the formation of the active species is a photoactivated process. Stirring the photocatalysis mixture in the dark for 4 h prior to irradiation did not result in a shorter induction period.

TEM of the particles after photocatalysis revealed aggregates of ∼100 nm that retained a nanocrystalline morphology (Fig. 4), but no additional features due to Co species (*e.g.* Co^0 nano-particles) were detected. Neither changes in the crystal phase of the CdS nor formation of additional phases were observable by XRD (Fig. S3†). We were unable to determine the oxidation state of the active Co species since the loading of Co was below the detection limit of X-ray photoelectron spectroscopy (XPS).

The oxidation state of bulk and surface CdS may also play an important role in catalysis. A comparison of XPS data for QD-OA, QD–BF$_4$ and QD–BF$_4$/CoCl$_2$ indicated changes in the QD surface chemistry during both ligand stripping and photo-catalysis. Firstly, there is a change in the stoichiometry of the particles during ligand-stripping, with QD-OA found to be Cd-rich (Cd : S = 0.63 : 0.37), whereas QD–BF$_4$ was almost stoi-chiometric (Cd : S = 0.53 : 0.47) and remained so during pho-tocatalysis (Table 2). The Cd(3d) peaks of QD-OA were

This journal is © The Royal Society of Chemistry 2016

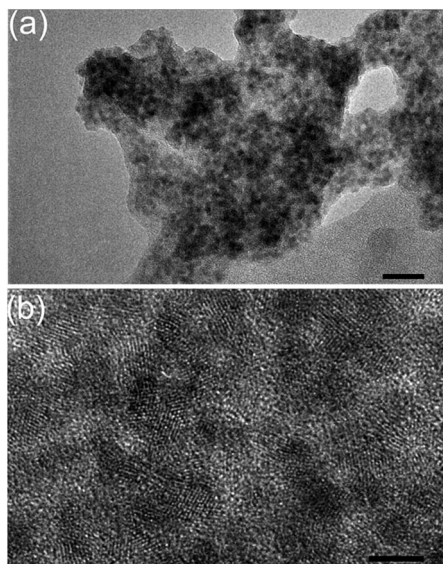*J. Mater. Chem. A*, 2016, **4**, 2856–2862 | **2859**

Fig. 4 TEM images of precipitates isolated from QD-BF$_4$/CoCl$_2$ after 4 h irradiation, showing (a) the aggregated, microscale structure (scale bar = 20 nm) and (b) nanocrystalline fine structure (scale bar = 5 nm).

Fig. 5 XPS spectra of S(2p) from QD-OA and QD-BF$_4$ particles and QD-BF$_4$ after photocatalysis with and without CoCl$_2$ as a co-catalyst.

broadened compared with those of QD-BF$_4$ (Fig. S10 and S11†), and could be fit to two spin-split peaks (3d$_{5/2}$ and 3d$_{3/2}$) consistent with bulk CdS (412.1 and 405.3 eV) and surface sulfur vacancies (410.7 and 403.9 eV).[53–57] Secondly, the S(2p) spectra for QD-BF$_4$ exhibit peaks corresponding to metal sulfide and metal sulfate (161.6 and 168.7 eV, respectively), indicating that the surface is partially oxidised (Fig. 5).[58] After photocatalysis, the proportion of sulfate remains approximately the same for QD-BF$_4$ alone (32.7 and 30.3% before and after photocatalysis, respectively), but decreases significantly in the presence of Co (17.9% and 10.5% after 12 h and 107 h, respectively; Table 2).

Since sulfate is the expected product of both photocorrosion of CdS and oxidation of the electron donor, SO$_3^{2-}$,[49] it is difficult to determine the origin of these signals. However, the change in stoichiometry and appearance of sulfate during ligand stripping is consistent with etching and the observed change in particle size. Since the subsequent loss of sulfate during photocatalysis is only observed in samples containing Co, it may either be a result of the Co incorporation (e.g. changes in the surface due to Co binding) or be indicative of the nature of the mechanism of activity enhancement (e.g. suppression of photocorrosion).

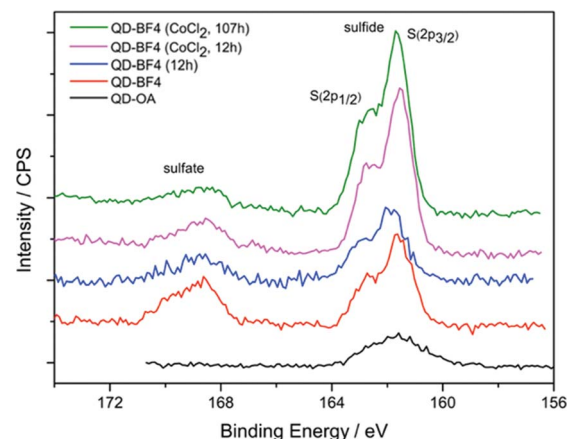The activity-enhancing role of the cobalt in this system is not entirely clear. Since no Cd was detected in the supernatant of the centrifuged photocatalysis reaction solution, it is unlikely that a significant proportion of the Co is integrated within the CdS particles by cation exchange. Although we cannot rule out that Co may be incorporated into interstitial Cd vacancies, the primary site for Co attachment is likely to be at the surface, consistent with previous studies of the photooxidative behaviour of CdS in the presence of Co ions,[59] and the sulfate displacement observed by XPS. The Co may either be deposited on the surface as an active catalyst species (e.g. Co$_x$S$_y$ or Co$_x$O$_y$)[47,60] or, alternatively, be adsorbed to the surface as Co ions (e.g. at surface hydroxyl or SO$_x^{2-}$ sites), behaving as charge-trapping sites to increase charge-separation and/or promote catalysis on the CdS surface.[61]

Since the required loading of Co for optimal activity is only two Co ions per QD, the formation of appreciably large domains of an active catalyst species on individual particles is unlikely. However, since the particles are agglomerated, one or more regions of such species might form on the surfaces of particle agglomerates. In this case, there may be many individual QDs with no Co physically attached but which form a conductive network and act as antennae, generating and conducting electrons towards remote active catalyst sites. This mechanism may be one reason why increasing the loading of Co does not increase the activity, since the surface area of the agglomerates is lower than of the individual particles. A corollary of this antenna hypothesis is that agglomeration of the QDs is in fact beneficial for H$_2$ production activity by facilitating charge

Table 2 Quantitative XPS analysis of Cd and S and relative sulfate and sulfide content of CdS QD before and after ligand stripping and after photocatalysis in the presence and absence of CoCl$_2$

Condition	Cd/at%	S/at%	Sulfide/% of S	Sulfate/% of S
QD-OA	63.1 ± 0.2	36.9 ± 0.9	100 ± 0	—
QD-BF$_4$	53.7 ± 0.2	46.3 ± 0.2	67.3 ± 2.3	32.7 ± 2.3
QD-BF$_4$, 12 h	51.8 ± 0.8	48.1 ± 0.8	69.7 ± 2.6	30.3 ± 2.6
QD-BF$_4$/CoCl$_2$, 12 h	52.8 ± 1.9	47.2 ± 1.9	82.1 ± 4.6	17.9 ± 4.6
QD-BF$_4$/CoCl$_2$, 107 h	54.1 ± 1.2	45.9 ± 1.2	89.5 ± 2.6	10.5 ± 2.6

2860 | J. Mater. Chem. A, 2016, 4, 2856–2862

This journal is © The Royal Society of Chemistry 2016

separation and retarding recombination, as has been shown for H_2 production on dye-sensitised, platinised TiO_2 nanoparticle powders.[62] Since agglomeration has also been reported with the highly active $CdTe/CoCl_2$ (microsphere) and $CdSe/Ni(DHLA)_2$ systems at pH 4–5,[25,28] we view this mechanism as an important consideration.

Based on our analysis of the active photocatalyst, we propose that the primary detrimental role of MPA in the QD-MPA/Co system is as a physical barrier. Since thiols do not dissociate from the particles as readily at pH 7 compared to pH 5 and below,[35,36] few surface sites on QD-MPA become available during the photoreaction, restricting incorporation of Co onto the particles and limiting substrate/product diffusion to and from the QD surface. The presence of MPA also prevents the particles from aggregating, possibly hindering efficient charge-separation. Finally, we avoid sequestration of Co by MPA, a secondary factor limiting the activity of thiol-capped QD systems.[27]

Conclusions

We have established ligand stripping as a facile and highly effective method to activate QDs in photocatalytic schemes, which allowed us to construct a QD/Co hybrid system with an unprecedented photoactivity in pH neutral solution. The active system consists of aggregates of stripped – and therefore surface-exposed – CdS particles with an attached cobalt species to enhance catalytic turnover. The photocatalyst system is active for several days, with the buffering ability of the electron donor as the main limiting factor. We anticipate that this approach can also be applied to a wide range of QDs, catalysts and redox transformations.

Acknowledgements

Notes and references

1 T. Faunce, S. Styring, M. R. Wasielewski, G. W. Brudvig, A. W. Rutherford, J. Messinger, A. F. Lee, C. L. Hill, H. deGroot, M. Fontecave, D. R. MacFarlane, B. Hankamer, D. G. Nocera, D. M. Tiede, H. Dau, W. Hillier, L. Wang and R. Amal, *Energy Environ. Sci.*, 2013, **6**, 1074–1076.

2 J. R. McKone, N. S. Lewis and H. B. Gray, *Chem. Mater.*, 2014, **26**, 407–414.

3 Y. Tachibana, L. Vayssieres and J. R. Durrant, *Nat. Photonics*, 2012, **6**, 511–518.

4 K. Maeda, M. Higashi, D. Lu, R. Abe and K. Domen, *J. Am. Chem. Soc.*, 2010, **132**, 5858–5868.

5 C. A. Caputo, M. A. Gross, V. W. Lau, C. Cavazza, B. V. Lotsch and E. Reisner, *Angew. Chem., Int. Ed.*, 2014, **53**, 11538–11542.

6 M. A. Gross, A. Reynal, J. R. Durrant and E. Reisner, *J. Am. Chem. Soc.*, 2014, **136**, 356–366.

7 K. Maeda and K. Domen, *J. Phys. Chem. Lett.*, 2010, **1**, 2655–2661.

8 M. B. Wilker, K. J. Schnitzenbaumer and G. Dukovic, *Isr. J. Chem.*, 2012, **52**, 1002–1015.

9 F. E. Osterloh, *Chem. Soc. Rev.*, 2013, **42**, 2294–2320.

10 F. E. Osterloh, *Chem. Mater.*, 2008, **20**, 35–54.

11 J. Sabaté, S. Cervera-March, R. Simarro and J. Giménez, *Int. J. Hydrogen Energy*, 1990, **15**, 115–124.

12 N. Bühler, K. Meier and J. F. Reber, *J. Phys. Chem.*, 1984, **88**, 3261–3268.

13 J. F. Reber and M. Rusek, *J. Phys. Chem.*, 1986, **90**, 824–834.

14 K. Kalyanasundaram, E. Borgarello, D. Duonghong and M. Grätzel, *Angew. Chem., Int. Ed.*, 1981, **20**, 987–988.

15 W. Zhang, Y. Wang, Z. Wang, Z. Zhong and R. Xu, *Chem. Commun.*, 2010, **46**, 7631–7633.

16 L. Huang, X. Wang, J. Yang, G. Liu, J. Han and C. Li, *J. Phys. Chem. C*, 2013, **117**, 11584–11591.

17 L. Huang, J. Yang, X. Wang, J. Han, H. Han and C. Li, *Phys. Chem. Chem. Phys.*, 2013, **15**, 553–560.

18 K. A. Brown, S. Dayal, X. Ai, G. Rumbles and P. W. King, *J. Am. Chem. Soc.*, 2010, **132**, 9672–9680.

19 K. A. Brown, M. B. Wilker, M. Boehm, G. Dukovic and P. W. King, *J. Am. Chem. Soc.*, 2012, **134**, 5627–5636.

20 M. B. Wilker, K. E. Shinopoulos, K. A. Brown, D. W. Mulder, P. W. King and G. Dukovic, *J. Am. Chem. Soc.*, 2014, **136**, 4316–4324.

21 B. L. Greene, C. A. Joseph, M. J. Maroney and R. B. Dyer, *J. Am. Chem. Soc.*, 2012, **134**, 11108–11111.

22 C.-B. Li, Z.-J. Li, S. Yu, G.-X. Wang, F. Wang, Q.-Y. Meng, B. Chen, K. Feng, C.-H. Tung and L.-Z. Wu, *Energy Environ. Sci.*, 2013, **6**, 2597–2602.

23 F. Wang, W.-J. Liang, J.-X. Jian, C.-B. Li, B. Chen, C.-H. Tung and L.-Z. Wu, *Angew. Chem., Int. Ed.*, 2013, **52**, 8134–8138.

24 F. Wang, W.-G. Wang, X.-J. Wang, H.-Y. Wang, C.-H. Tung and L.-Z. Wu, *Angew. Chem., Int. Ed.*, 2011, **50**, 3193–3197.

25 Z.-J. Li, X.-B. Li, J.-J. Wang, S. Yu, C.-B. Li, C.-H. Tung and L.-Z. Wu, *Energy Environ. Sci.*, 2013, **6**, 465–469.

26 C. Gimbert-Suriñach, J. Albero, T. Stoll, J. Fortage, M.-N. Collomb, A. Deronzier, E. Palomares and A. Llobet, *J. Am. Chem. Soc.*, 2014, **136**, 7655–7661.

27 A. Das, Z. Han, M. G. Haghighi and R. Eisenberg, *Proc. Natl. Acad. Sci. U. S. A.*, 2013, **110**, 16716–16723.

28 Z. Han, F. Qiu, R. Eisenberg, P. L. Holland and T. D. Krauss, *Science*, 2012, **338**, 1321–1324.

29 Z.-J. Li, X.-B. Fan, X.-B. Li, J.-X. Li, C. Ye, J.-J. Wang, S. Yu, C.-B. Li, Y.-J. Gao, Q.-Y. Meng, C.-H. Tung and L.-Z. Wu, *J. Am. Chem. Soc.*, 2014, **136**, 8261–8268.

30 T. Simon, N. Bouchonville, M. J. Berr, A. Vaneski, A. Adrović, D. Volbers, R. Wyrwich, M. Döblinger, A. S. Susha,

This journal is © The Royal Society of Chemistry 2016

J. Mater. Chem. A, 2016, **4**, 2856–2862 | **2861**

A. L. Rogach, F. Jäckel, J. K. Stolarczyk and J. Feldmann, *Nat. Mater.*, 2014, **13**, 1013–1018.

31 F. Lakadamyali, M. Kato, N. M. Muresan and E. Reisner, *Angew. Chem., Int. Ed.*, 2012, **51**, 9381–9384.

32 T. W. Kim and K.-S. Choi, *Science*, 2014, **343**, 990–994.

33 M. A. Holmes, T. K. Townsend and F. E. Osterloh, *Chem. Commun.*, 2012, **48**, 371–373.

34 K. P. Acharya, R. S. Khnayzer, T. O'Connor, G. Diederich, M. Kirsanova, A. Klinkova, D. Roth, E. Kinder, M. Imboden and M. Zamkov, *Nano Lett.*, 2011, **11**, 2919–2926.

35 J. Aldana, N. Lavelle, Y. Wang and X. Peng, *J. Am. Chem. Soc.*, 2005, **127**, 2496–2504.

36 M. J. Mulvihill, S. E. Habas, I. Jen-La Plante, J. Wan and T. Mokari, *Chem. Mater.*, 2010, **22**, 5251–5257.

37 F. Lakadamyali and E. Reisner, *Chem. Commun.*, 2011, **47**, 1695–1697.

38 E. L. Rosen, R. Buonsanti, A. Llordes, A. M. Sawvel, D. J. Milliron and B. A. Helms, *Angew. Chem., Int. Ed.*, 2012, **51**, 684–689.

39 W. W. Yu, L. Qu, W. Guo and X. Peng, *Chem. Mater.*, 2003, **15**, 2854–2860.

40 J. Liu, X. Yang, K. Wang, D. Wang and P. Zhang, *Chem. Commun.*, 2009, 6080–6082.

41 F. Lakadamyali, A. Reynal, M. Kato, J. R. Durrant and E. Reisner, *Chem.–Eur. J.*, 2012, **18**, 15464–15475.

42 J. Willkomm, N. M. Muresan and E. Reisner, *Chem. Sci.*, 2015, **6**, 2727–2736.

43 B. S. Veldkamp, W.-S. Han, S. M. Dyar, S. W. Eaton, M. A. Ratner and M. R. Wasielewski, *Energy Environ. Sci.*, 2013, **6**, 1917–1928.

44 D. W. Wakerley and E. Reisner, *Phys. Chem. Chem. Phys.*, 2014, **16**, 5739–5746.

45 N. M. Muresan, J. Willkomm, D. Mersch, Y. Vaynzof and E. Reisner, *Angew. Chem., Int. Ed.*, 2012, **51**, 12749–12753.

46 L. A. Berben and J. C. Peters, *Chem. Commun.*, 2010, **46**, 398–400.

47 S. Cobo, J. Heidkamp, P.-A. Jacques, J. Fize, V. Fourmond, L. Guetaz, B. Jousselme, V. Ivanova, H. Dau, S. Palacin, M. Fontecave and V. Artero, *Nat. Mater.*, 2012, **11**, 802–807.

48 T. M. McCormick, B. D. Calitree, A. Orchard, N. D. Kraut, F. V. Bright, M. R. Detty and R. Eisenberg, *J. Am. Chem. Soc.*, 2010, **132**, 15480–15483.

49 D. Meissner, R. Memming and B. Kastening, *J. Phys. Chem.*, 1988, **92**, 3476–3483.

50 P. Neta and R. E. Huie, *Environ. Health Perspect.*, 1985, **64**, 209–217.

51 Y. Xu and M. A. A. Schoonen, *Am. Mineral.*, 2000, **85**, 543–556.

52 A. Reynal, E. Pastor, M. A. Gross, S. Selim, E. Reisner and J. R. Durrant, *Chem. Sci.*, 2015, DOI: 10.1039/c5sc01349f.

53 Y.-M. Fang, J. Song, R.-J. Zheng, Y.-M. Zeng and J.-J. Sun, *J. Phys. Chem. C*, 2011, **115**, 9117–9121.

54 A. Veamatahau, B. Jiang, T. Seifert, S. Makuta, K. Latham, M. Kanehara, T. Teranishi and Y. Tachibana, *Phys. Chem. Chem. Phys.*, 2015, **17**, 2850–2858.

55 J. F. Moulder, W. F. Stickle, P. E. Sobol and K. D. Bomben, *Handbook of X-ray Photoelectron Spectroscopy*, Physical Electronics Inc., Minnesota, USA, 1992.

56 H. L. Lee, A. M. Issam, M. Belmahi, M. B. Assouar, H. Rinnert and M. Alnot, *J. Nanomater.*, 2009, 914501.

57 S. Rengaraj, S. Venkataraj, S. H. Jee, Y. Kim, C.-w. Tai, E. Repo, A. Koistinen, A. Ferancova and M. Sillanpää, *Langmuir*, 2011, **27**, 352–358.

58 J. I. Kim, J. Kim, J. Lee, D.-R. Jung, H. Kim, H. Choi, S. Lee, S. Byun, S. Kang and B. Park, *Nanoscale Res. Lett.*, 2012, **7**, 482–488.

59 Y. H. Hsieh, C. P. Huang and A. P. Davis, *Chemosphere*, 1992, **24**, 281–290.

60 C.-Y. Lin, D. Mersch, D. A. Jefferson and E. Reisner, *Chem. Sci.*, 2014, **5**, 4906–4913.

61 S. R. Pendlebury, X. Wang, F. Le Formal, M. Cornuz, A. Kafizas, S. D. Tilley, M. Grätzel and J. R. Durrant, *J. Am. Chem. Soc.*, 2014, **136**, 9854–9857.

62 Y. Park, W. Kim, D. Monllor-Satoca, T. Tachikawa, T. Majima and W. Choi, *J. Phys. Chem. Lett.*, 2013, **4**, 189–194.

2862 | *J. Mater. Chem. A*, 2016, **4**, 2856–2862

This journal is © The Royal Society of Chemistry 2016